

## Performance of cavity backed inverted microstrip broadband antenna

Sheikh Sharif Iqbal<sup>1</sup>, Manotosh Biswas<sup>2</sup>, Jawad Y. Siddiqui<sup>2</sup> & Debatosh Guha<sup>3</sup>

<sup>1</sup>E E Department, King Fahd University of Petroleum and Minerals, Dhahran, Saudi Arabia  
e-mail: sheikhsi@kfupm.edu.sa

<sup>2</sup>Institute of Radio Physics and Electronics, University of Calcutta, Calcutta 700 009, India

<sup>3</sup>Department of ECE, Royal Military College Of Canada, PO Box 17000, Station Forces CP 17000,  
Kingston, Ontario K7K 784, Canada

Received 17 May 2005; revised 30 November 2005; accepted 15 December 2005

An inverted microstrip circular patch with a parasitic element printed back-to-back on the same substrate and backed by a cylindrical metallic cavity is investigated as a compact integratable broadband antenna. The cavity effect in changing its impedance behaviour is thoroughly examined and an optimized X-band design is presented. As much as 11% bandwidth is apparent from the design data. Principal plane radiation patterns are also examined, showing above 98% efficiency and 10.97 dB directivity.

**Keywords:** Microstrip antenna, Stacked patch antenna, Cavity backed antenna, Broadband antenna

**PACS No.:** 84.40.Ba

**IPC Code:** H01Q9/00; H01Q21/00; H01Q23/00

### 1 Introduction

The inverted microstrip circular patch (IMCP) backed by a cylindrical cavity was experimentally investigated by Chang *et al.*<sup>1-3</sup> to develop a series of integrated antenna modules. The advantage of the inverted microstrip geometry shown in Fig. 1, is mainly caused by the air dielectric existing in between the inverted patch and the ground plane. This allows easy integration of active devices with patch and also easy optimization of the feed location in a probe-fed design without any degradation of the medium. The structure is also free from surface wave generation.

The advantageous features and applications of the inverted microstrip geometry have generated a lot of interest in recent years. Computer aided designs of an IMCP in open-to-air geometry (Fig. 1) have been reported by Guha and Siddiqui.<sup>4-5</sup> They also have analyzed<sup>6</sup> the effect of a cylindrical cavity backing on the operating frequency of an IMCP. Single element open-to-air IMCP shown in Fig. 1 can offer nearly 4% –10 dB return loss bandwidth.<sup>5</sup> The improvement of the impedance bandwidth can make the antenna more suitable for integrated antenna applications, particularly where the same antenna can be used in transmit and receive modes at two frequencies. The present authors have already studied the performance of an

open-to-air IMCP loaded with a parasitic patch as a broadband antenna.<sup>7-8</sup> The effect of a cylindrical cavity backing yet another area of investigation, since this antenna either in a probe-fed or in an integrated form demands a compactness in terms of ground plane dimension, good shielding and high gain with handy configuration. A metallic cavity backing provides all these effects.<sup>2,6</sup>

In this paper, we have studied the performance of a cavity backed stacked IMCP (CB-SIMCP) as shown in Fig. 2 and have simultaneously optimized the antenna and cavity dimensions to obtain the optimum input impedance characteristics. Though the cavity

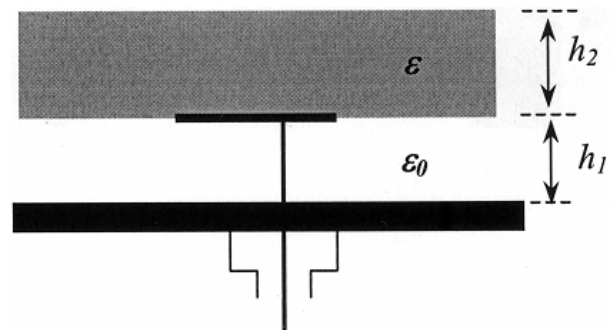


Fig. 1—Probe-fed inverted microstrip antenna in open-to-air geometry.

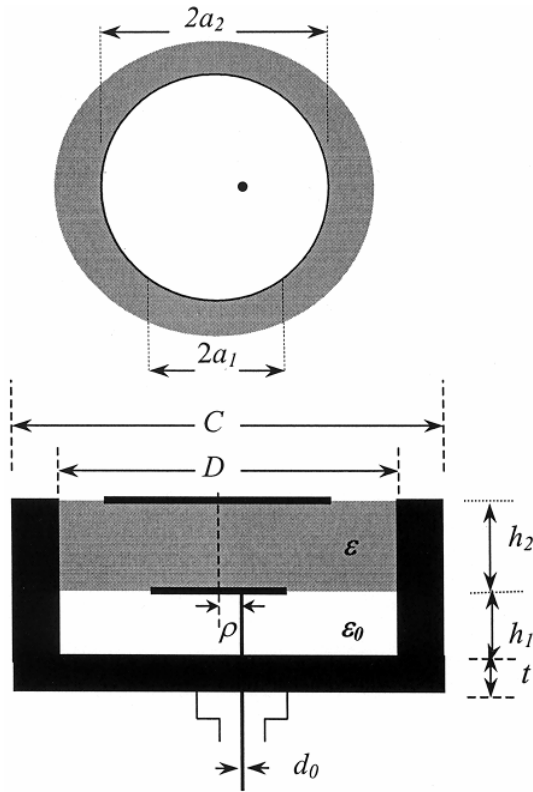


Fig. 2—Cavity backed stacked inverted microstrip circular patch antenna.

backed stacked rectangular<sup>9</sup> and circular<sup>10</sup> patch have been investigated earlier as broadband antennas, the proposed design differs from the previous ones in various aspects: (i) The present design employs a single substrate and hence is free from the mis-alignment of patches, (ii) It is low cost, low volume and compact in shape, (iii) Unlike all previous designs, the proposed antenna is integratable with active devices like Gunn and varactor diodes.<sup>1,2</sup> Commercial HFSS full wave solver is used to generate the design data and to study the antenna performance. As large as 11% bandwidth with 11 dB directivity and good radiation patterns are reported.

## 2 The antenna geometry

A cavity backed IMCP (CB-IMCP) with a parasitic patch loading on its upper face is shown in Fig. 2. The metallic cavity is of cylindrical size and the dimensional parameters are indicated in Fig. 2. The figure shows the concentric alignment of the patches.

The approximate operating frequency of this type of antenna can be estimated employing the CAD formulas<sup>4</sup> for single element IMCP (Fig. 1). Such estimation has already been successfully tested.<sup>8</sup> The patch

radius  $a_1$  was calculated as 5.5 mm without considering the effect of the parasitic element  $a_2$ , to operate the antenna approximately at 12 GHz. The upper patch dimension  $a_2 = 1.45 \times a_1$  has been tested to achieve the optimum input impedance behaviour.<sup>8</sup> The parameters  $h_1$ ,  $h_2$ , and  $\epsilon_r$  are chosen as 1.6 mm, 1.575 mm, and 2.33 mm, respectively as typical commercial values for design purpose. The diameters of the inner and outer conductors of the feeding probe are taken as 0.245 mm and 2.1 mm, respectively for commercially available SMA feeds.

## Antenna characteristics

The input impedance, bandwidth and radiation characteristics of the CB-SIMCP antenna are examined with the help of the simulated data obtained by using the HFSS full wave solver version. The simulated results can be reliably used to design the new antenna since its predicted values for alike microstrip antennas were experimentally verified earlier.<sup>8,11</sup> The input impedance behaviour of the antenna is examined from its return loss versus frequency trace. This also gives information about the resonance frequency and operating bandwidth for a specified return loss value.

Figure 3(a) shows the simulated return loss versus frequency curves of a S-IMCP enclosed in a cavity having diameter  $D = 1.73 \times 2a_1$  and coaxially fed at different radial locations  $\rho$ . Three different  $\rho$  values with  $\rho/a_1 = 0.36, 0.73$  and  $0.95$  result in different return loss characteristics. These are completely different from those for an identical open-to-air S-IMCP as shown in Fig. 3(b). The data of Fig. 3(b) are generated just by removing the cavity wall from Fig. 2, keeping the ground plane and the substrate dimensions same as in case of Fig. 3(a). The  $S_{11}$  minimum for the  $TM_{11}$  mode gradually shifts to the higher frequency side of the spectrum as  $\rho/a_1$  increases and each of them is below  $-10$  dB. Moreover, the traces indicate larger impedance bandwidth as  $\rho/a_1$  increases. The return loss characteristics of Fig. 3(a) appears to be somewhat complicated compared to those of Fig. 3(b) and this is caused by the presence of the cavity wall surrounding the patch. The new features may be noted as: (a)  $\rho/a_1 = 0.36$  results in a second resonance centered at 13 GHz and this is totally absent for  $\rho/a_1 \approx 0.95$ , (b) intermediate and large  $\rho/a_1$  values (0.73 and 0.95, respectively) show no  $S_{11}$  value below  $-10$  dB. Hence, the effect of the cavity diameter on the input impedance behaviour of an S-IMCP is examined in

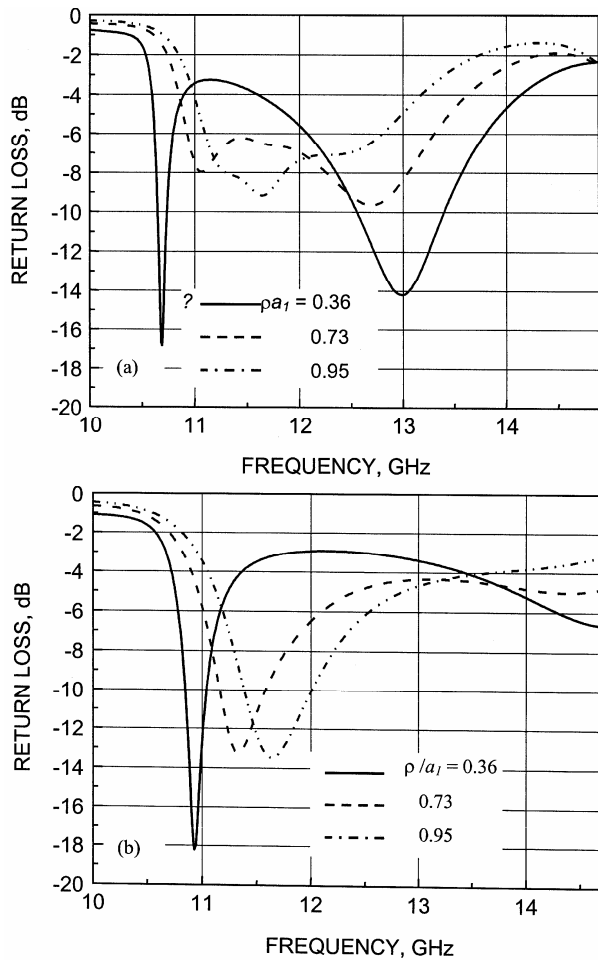


Fig. 3—Return loss versus frequency of a SIMCP with different feed locations (a) Cavity backed (b) Open-to-air [ $\epsilon_r = 2.33$ ,  $D/2a_1 = 1.73$ ,  $a_1 = 5.5$ ,  $a_2 = 8.0$ ,  $h_1 = 1.6$ ,  $h_2 = 1.575$ ,  $t = 1.855$ ,  $C = (D+9)$  (all dimensions in mm)]

Fig. 4 by varying  $D/2a_1$  values from 1.56 to 2.8. Small  $\rho/a_1$  is chosen to examine the dominant mode along with the second resonance near 13 GHz. Smaller the cavity diameter, narrower the impedance bandwidth of the dominant mode. Large cavity with  $D/2a_1 = 2.8$  results in no resonance at 13 GHz, but this occurs when  $D/2a_1 \leq 1.73$  and in that case, smaller cavity indicates lower  $S_{11}$  minima at resonance.

Thus the 13 GHz resonance is very much influenced by the proximity of the cavity wall with respect to the patch boundary and for academic interest, the nature of the resonating mode is examined in an interesting way in Fig. 5. In Fig. 5, small cavity with  $D/2a_1 = 1.56$  is chosen with  $\rho/a_1 = 0$  and 0.36. The centrally located probe with  $\rho/a_1 = 0$  shows no  $TM_{11}$  resonance as it is hardly supported by the probe near  $\rho \approx 0$ . Rather, this  $\rho$  value is suitable for exciting

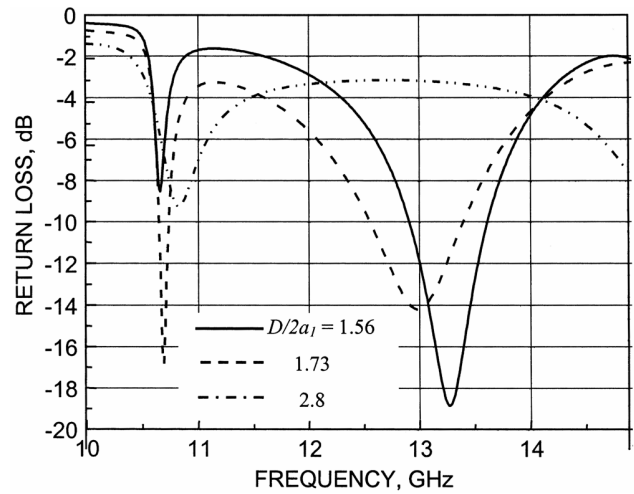


Fig. 4—Return loss versus frequency of a CB-SIMCP antenna with different cavity diameters ( $\rho/a_1 = 0.36$ , other parameters as in Fig. 3)

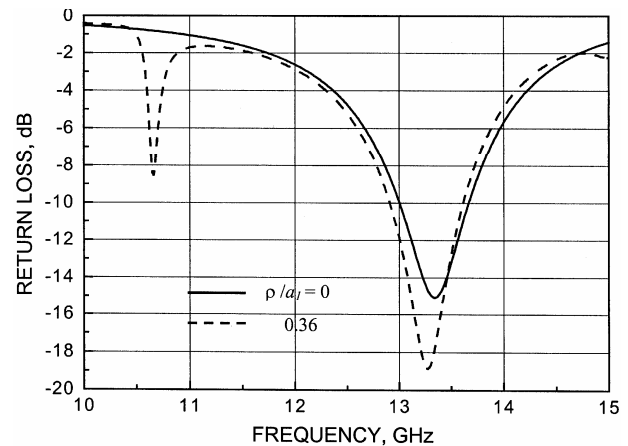


Fig. 5—Return loss versus frequency of a CB-SIMCP antenna with different feed locations ( $D/2a_1 = 1.56$ , other parameters as in Fig. 3)

$TM_{01}$  mode, which is confirmed by its simulated radiation patterns (not shown here). This also matches the dominant resonating mode of a circular cavity itself.

So in case of an antenna, large  $D/2a_1$  with large  $\rho/a_1$  value is desirable from the point of view of  $TM_{11}$  resonance with larger bandwidth. This has been thoroughly examined for  $\rho/a_1 = 0.95$  in Fig. 6. The  $S_{11}$  curve for  $D/2a_1 = 1.73$  shows a pattern of overcoupling caused by the parasitic patch.<sup>8</sup> This ultimately is favourably grown by the cavity walls and an optimum response is obtained when  $D/2a_1 = 2.8$ . As much as 11% bandwidth ( $S_{11} < -10$  dB) is apparent from this design, which for an identical open-to-air geometry can be as large as 6%, as depicted in Fig. 7.

The radiation characteristics of the CB-SIMCP antennas are examined in Fig. 8 for different cavity diameters already explained in Fig. 6. Indeed, Figs 8 (a) and (b) correspond to the return loss curves ‘a’ and ‘b’ of Fig. 6. Radiation patterns for  $D/2a_1 = 2.8$  (return loss curve a) shows improved directivity in both the planes compared to those produced by smaller cavity

diameter with  $D/2a_1 = 1.9$ . Moreover, the larger cavity shows very much improved cross-polarization characteristics over the operating angles. This is also true that the cross-polarization levels appearing in H-plane attributes no disqualification to the antenna patterns, as this is basically used for mobile communication.

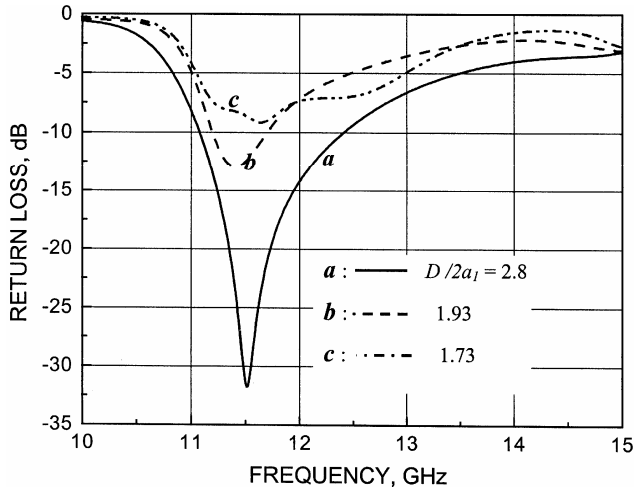


Fig. 6—Return loss versus frequency of a CB-SIMCP antenna with different cavity diameters ( $\rho/a_1 = 0.95$ , other parameters as in Fig. 3)

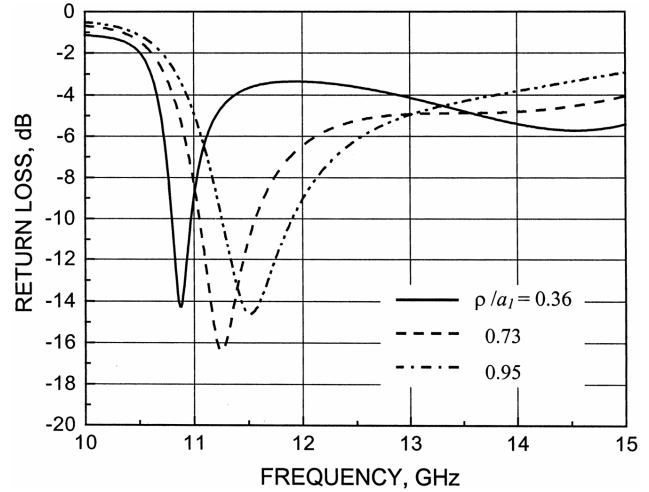


Fig 7—Return loss versus frequency of an open-to-air SIMCP antenna with different feed locations ( $D/2a_1 = 2.8$ , other parameters as in Fig. 6)

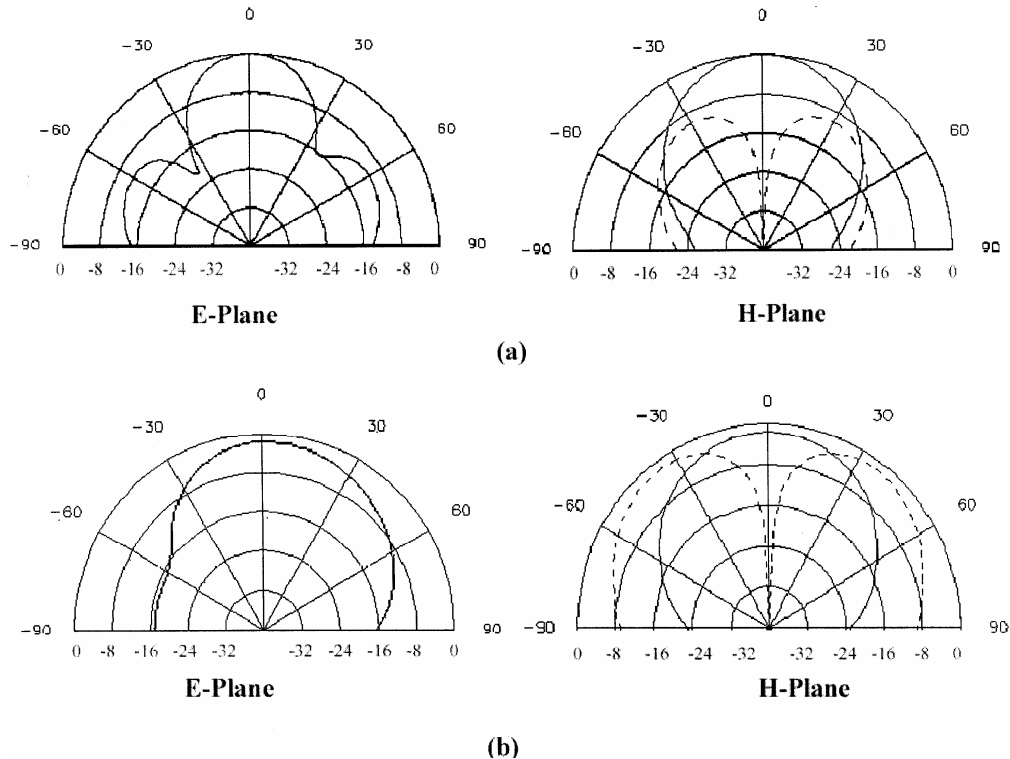


Fig. 8—Principal plane radiation patterns of the CB-SIMCP antennas investigated in Fig. 6 (— Co-Polarization, ---- Cross-Polarization [(a)  $D/2a_1 = 2.8, f = 11.5$  GHz, (b)  $D/2a_1 = 1.9, f = 11.45$  GHz])

#### 4 Conclusions

A cavity backed inverted microstrip circular patch loaded with a parasitic element is designed as a broadband integratable antenna. An optimum design in X-band is presented. The preliminary design frequency is well within the operating band. As much as 11% dominant mode bandwidth is obtained from a compact low cost antenna. The cavity enclosure helps in enhancing the impedance bandwidth over and above that obtained from an open-to-air structure. Possibility of nearly 85% improvement is evident from the simulated design data. The radiation patterns also show its suitability in developing a broadband active or probe-fed antenna for portable communication equipment.

#### Acknowledgement

The authors are grateful for the partial support extended by the King Fahd University of Petroleum and Minerals (KFUPM), Dhahran, Saudi Arabia and the CAS in the Institute of Radio Physics and Electronics, University of Calcutta, Kolkata, India.

#### References

- 1 Flynt R A, Fan L, Navarro J A & Chang K, *IEEE Trans Microwave Theory and Tech (USA)*, MTT-44 (1996) 1642.
- 2 Navarro J A, Fan L & Chang K, *IEEE Trans Microwave Theory and Tech (USA)*, MTT-41 (1993) 1856.
- 3 Navarro J A, Fan L & Chang K, *Electron Lett (UK)*, 30 (1994) 655.
- 4 Guha D & Siddiqui J Y, *Microwave Opt Technol Lett (USA)*, 35-6 (2002) 434.
- 5 Siddiqui J Y & Guha D, *Microwave Opt Technol Lett*, 39-6 (2003) 508
- 6 Guha D & Siddiqui J Y, *IEEE Trans on Antennas Propag (USA)*, 52-8 (2004) 2177.
- 7 Siddiqui J Y, Guha D & Iqbal Sheikh S, Input Impedance Behaviour of Coax-fed Inverted Microstrip Stacked Patches, *Proc Int Conf on Communication, Devices and Intelligent Systems*, Calcutta, India, (2004), 220.
- 8 Sheikh S I, Siddiqui J Y & Guha D, *Electromagnetics (USA)*, 25-4 (2005) 317.
- 9 Gonzalez de Aza M A, Zapata J & Encinar J A, *IEEE Trans Antennas Propag (USA)*, AP-48 (2000) 784.
- 10 Zavosh F & Aberle J T, *IEEE Trans Antennas Propag (USA)*, AP-43 (1995) 746.
- 11 Sheikh S Iqbal, Siddiqui J Y & Guha D, *IEEE Symp Antennas Propag (USA)*, 2 (2003) 288.